www.czasopisma.pan.pl PAN POLSKA AKADEMIA NAUK www.journals.pan.pl

Arch. Metall. Mater. **68** (2023), 2, 807-812

DOI: https://doi.org/10.24425/amm.2023.142465

J. LADE[1*], B. DHARAVATH[1], A. BADRISH[2], S. KOSARAJU[3], S.K. SINGH[3], K.K. SAXENA[4]

EVOLUTION AND CHARACTERIZATION OF ZIRCONIUM 702 ALLOY AT VARIOUS TEMPERATURES

The Zirconium 702 alloy effectively used in nuclear industry at various critical conditions like high temperature and high pressure. This survey is an assessment of insights into the mechanical properties of the metal when exposed to different temperatures along the rolling direction.The main objective of this work is to characterize the tensile properties, and fracture study of broken tensile test samples at various temperatures.The tensile samples tested in our current work are 100°C,150°C, and 200°C temperatures in different directions (0°, 45°, 90°) along with the rolling direction of the sheet. It is evident from the experimental results that temperatures significantly affect material properties. Temperature increases cause % elongation to increase, and strength decreases. ANOVA analysis revealed that temperature significantly influenced ultimate tensile strength (UTS), and yield strength (YS), as well as % elongation.The temperature contribution for UTS, YS, and % elongation is 41.90%, 31.60%, and 77.80% respectively. SEM fractured images showing the ductile type of behavior for all the temperatures.

Keywords: Zirconium 702 alloy; ANOVA; % elongation; Ultimate tensile strength; yield strength; scanning electron microscope

1. Introduction

A significant portion of nuclear power plants are constructed using zirconium alloys because of their strength, ductility, and resistance to corrosion at high temperatures [1-3]. Tin, iron, niobium, nickel, chromium, and other alloying elements give them these properties. In the 1950s, zirconium alloys were developed and new names, such as Zircaloy-1, Zircaloy-2, Zircaloy-3, and Zircaloy-4, were created to describe their properties. The corrosion resistance of Zircaloy-1 and Zircaloy-3 makes them obsolete. For this reason, zirconium alloys are widely used in nuclear applications.

The present work is focusing on the mechanical characterization of material under various testing conditions and also optimizing for finding the effective one. Optimizing the mechanical properties of the component is the key to increasing the production efficiency and maintaining quality, as well as achieving the commercial success of the component. Manufacturing processes need to be modeled to optimize them. In spite of the lack of a model to optimize the mechanical properties of materials, this article provides the best method. To reduce the time and cost of manufacturing, experimental methods such as Taguchi methods, factorial designs, and ANOVA are widely used [4-6]. Baloji et al. [7] developed an empirical model to describe the evolution of mechanical properties and validated numerical and experimental results using ANOVA.

In the recent past, Shuichi Miyazaki et al. [8] depict a zirconium composite that has such flexible properties that it is utilized in organic and clinical fields. The compound is used as flexible as human bones from obtained mechanical properties which makes it a suitable material for making artificial parts of the body like bones, teeth, stents, joints, and other surgical or clinical inserts making its first preferable material in the clinical fields. Zhang Y et al. [9] have studied the effect of strain rate and temperature on Cu-Cr-Zr alloy on the basis of simulations and experiments. Dunkerley et al. [10] determined the understanding of work-hardening and recrystallization is not only fundamental to the accomplishment of mechanical forming yet in addition essential to improving the microstructure and properties of the products. The distinct strain hardening phenomenon occurs under relatively lower temperatures. Swadesh et al. [11-17] worked on different materials like Austenitic steels, inconel, and zirconium alloys at various temperatures and they have determined mechanical properties, and formability behavior, and also optimized these properties

[1] KG REDDY COLLEGE OF ENGINEERING & TECHNOLOGY, DEPARTMENT OF MECHANICAL ENGINEERING, HYDERABAD 500075, INDIA
[2] DOFS,DRDL, HYDERABAD, 500058, INDIA
[3] GRIET, DEPARTMENT OF MECHANICAL ENGINEERING, HYDERABAD 500090, INDIA
[4] DIVISION OF RESEARCH AND DEVELOPMENT, LOVELY PROFESSIONAL UNIVERSITY, PHAGWARA 144411, INDIA

* Corresponding author: jayahari.lade@gmail.com

using various methods. The formability drastically increased at elevated temperatures with ductile type fracture in the sample.

This experimentation emphasizes the characterization of zirconium by tensile tests at different temperatures 100°C from to 250°C in the interval of 50°C at three constant strain rates. Different properties of the metal have been evaluated from the test data. A fracture study on the tensile test specimens has been carried out to study the material behavior at these temperatures.

2. Experimental details

2.1. Work material and chemical composition

A zirconium alloy, Zirconium 702 belongs to the zirconium family. Due to its corrosion resistance, zirconium is widely used in marine and chemical applications. Due to its high strength-to-weight ratio, it is also widely used in aircraft applications. TABLE 1 shows zirconium 702's chemical composition. Wire-cut electric discharge machining is used in this study to cut the tensile samples. Fig. 1 shows the samples are according to ASTM E8/E11 and taken at three orientations along the rolling direction of the sheet.

TABLE 1

Chemical composition of Zirconium 702 alloy

Element /Gas	Zirconium	Hafnium	Hydrogen	Carbon	Nitrogen	Oxygen
Weight %	97.66	2.34	0.005	0.05	0.025	0.16

2.2. Experimental design and test conditions

According to TABLE 2, the design matrix is based on a full factorial design with three factors: strain rate, orientation, and temperature. Tests were conducted randomly based on this design matrix TABLE 3.

2.3. Experimental setup

The uniaxial tensile test was conducted on a computerized Universal Testing Machine (UTM) with 20 ton capacity and connected with a heating furnace to maintain the required temperature during the test. The Experimental setup and tested samples are shown in Fig. 2.

TABLE 2

Experimentation Parameters and their levels

Factors	Units	Level-1	Level-2	Level-3
Strain rate	/s	0.1	0.01	0.001
Temperature	°C	100	150	200
Orientation	degree	0	45	90

TABLE 3

Arrangement of matrix and experimental results

Std	Run	Temperature (°C)	Orientation (Degree)	Strain rate (/s)	Yield strength (MPa)	Ultimate tensile strength (MPa)	% elongation
1	18	100	0	0.001	162.41	300.72	45.98
2	12	150	0	0.001	88.83	196.21	55.63
3	14	200	0	0.001	77.22	147.31	62.99
4	13	100	45	0.001	164.11	301.2	46.11
5	09	150	45	0.001	87.21	194.21	55.71
6	10	200	45	0.001	76.31	146.32	63.33
7	22	100	90	0.001	165.91	301.57	46.33
8	3	150	90	0.001	86.15	193.11	55.77
9	7	200	90	0.001	75.11	146.21	63.12
10	17	100	0	0.01	180.85	316.12	41.11
11	11	150	0	0.01	99.55	212.25	51.11
12	20	200	0	0.01	98.56	169.31	59.36
13	06	100	45	0.01	181.88	318.21	41.29
14	26	150	45	0.01	99.22	210.99	52.38
15	16	200	45	0.01	97.21	169.11	59.21
16	25	100	90	0.01	182.23	319.11	41.32
17	04	150	90	0.01	99.39	211.32	52.36
18	8	200	90	0.01	96.99	168.91	59.01
19	1	100	0	0.1	205.23	340.56	36.12
20	24	150	0	0.1	119.11	234.85	43.91
21	2	200	0	0.1	117.23	209.31	56.11
22	21	100	45	0.1	202.22	333.65	36.12
23	15	150	45	0.1	119.25	236.95	44.21
24	23	200	45	0.1	115.11	202.55	56.31
25	05	100	90	0.1	201.51	339.20	36.10
26	27	150	90	0.1	118.92	236.45	44.11
27	19	200	90	0.1	115.32	203.69	56.38

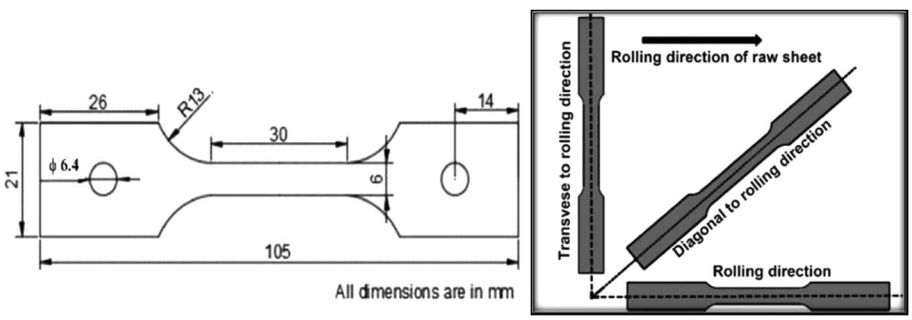

Fig. 1. ASTM E8/E11 standard Tensile specimen and representation of different orientations (0°, 45°, 90°)

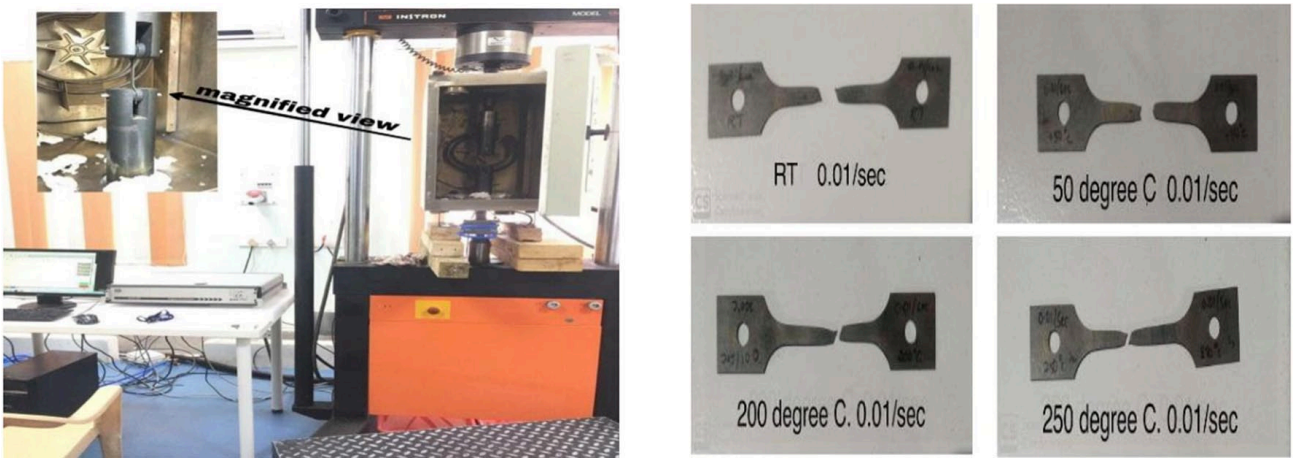

Fig. 2. Experimental setup for Computerized Universal Testing Machine and fractured samples at different temperature conditions

3. Results and discussions

3.1. Tensile behavior

Fig. 3(a,c) shows stress-plastic strain plots for Zirconium at different temperatures with a constant strain rate. With increasing test temperature, the flow stress decreases. Flow stress variation, however, is barely affected by strain rate variation. As small strains (up to 0.001) increase, true stress increases sharply, followed by a slow rise in flow stress until ultimate stress is reached. Macroscopic deformation was uniform, which contributed to the sharp rise in tensile strength. During the early stages of deforma-

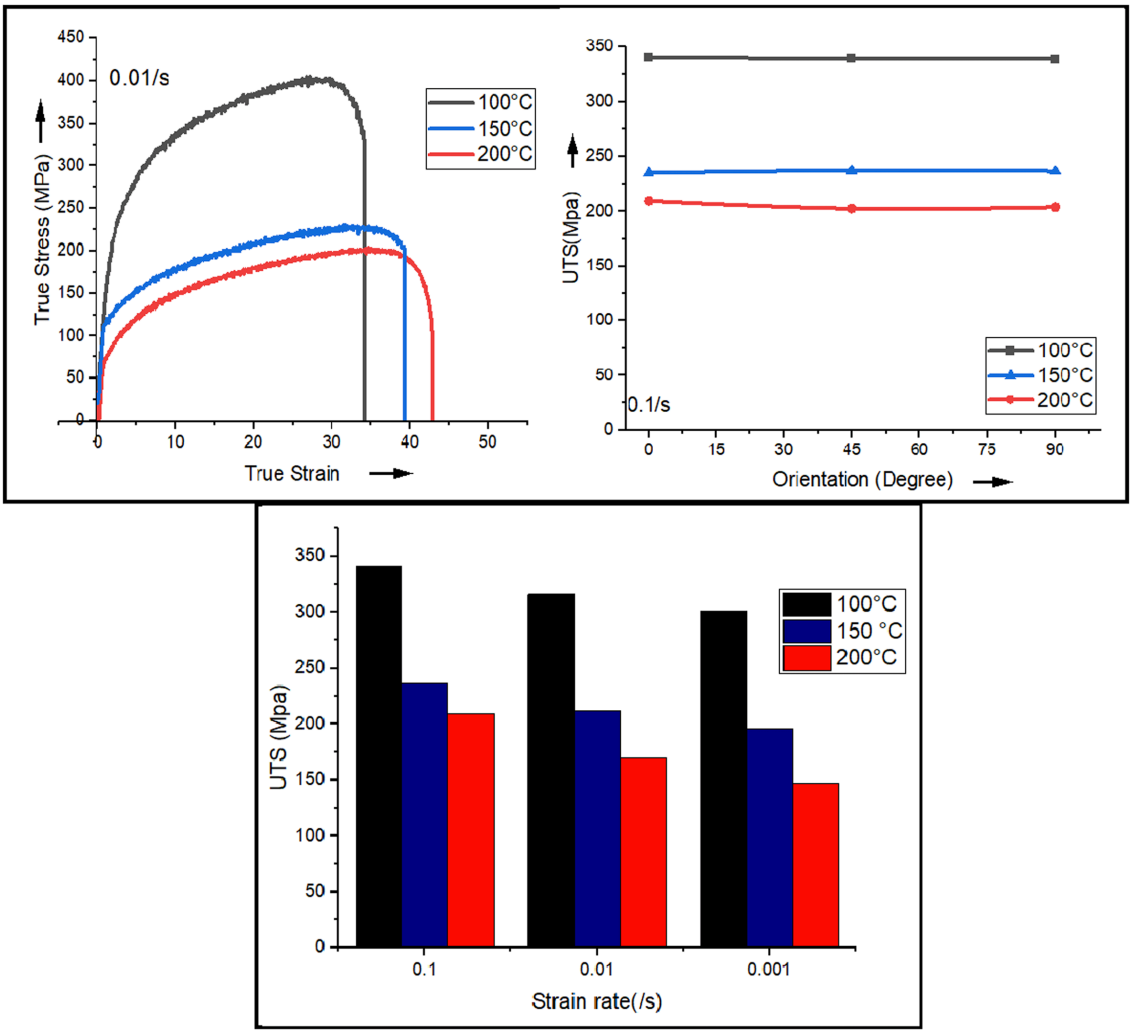

Fig. 3. (a) True Stress Vs True Strain curves at different temperatures at 0.01/sec, (b) Representation of UTS Vs Orientation at different temperatures and (c) Representation of UTS Vs strain rate at different temperatures

tion, dislocation mobility is mainly observed. As the deformation progresses, uniform deformation is usually followed by diffuse or localized necking and finally fracture [18]. The flow stress increases by increasing the strain rate from 0.001 to 0.1/s. Across the temperature range of 100-200°C, serrated flow stress has been observed for all strain rates. Generally, serrated yielding occurs when solute atoms migrate out faster than dislocation speed. As a result, locked dislocations increase load-carrying capacity. When dislocations overcome these solute atoms, a sudden load drop occurs. As a result of inhomogeneous deformation, the Portevin-Le Chatelier (PLC) phenomenon defines the serration [19]. Fig. 3(b) shows the variation of ultimate tensile strength with respect to orientation, very small variation was observed when samples fractured and in case rolling direction the UTS value is slightly high compared to other two directions.

3.2. SEM

The SEM images Fig. 4(a-c) of post-tensile fracture surfaces show equiaxed ductile dimples typical of ductile fracture surfaces. With an increase in temperature ridges (white portion shown with arrow) at 100°C, dimples (dark portion shown with arrow) at 150°C and 200°C were observed. These more dimples and flow lines were clearly declared ductile fractures. The flowability of the material increases while increasing test temperature and dimples at the fracture surface due to void growth and nucleation. The material becomes more ductile at higher temperatures. A decline in mean flow stress and a change in grain boundary flow behavior combined to produce this effect [20].

4. ANOVA

The experimental results were also analyzed by analysis of variance (ANOVA). Analyzing performance characteristics using ANOVA is designed to determine which process parameters significantly impact them. Temperature is the most significant control parameter for flow stress behavior, according to the percentage contribution shown in TABLE 4-6. In addition, a regression analysis was also performed for yield strength, ultimate strength, and elongation. It was observed that the R2 value for yield strength was 89.91%, for ultimate strength 96.51% and for elongation 96.47%. The R-squared statistic measures the distance between the fitted regression line and the data. Values closer to 100 are considered to be better.

TABLE 4

Analysis of Variance Yield Strength

Source	DF	Adj SS	Adj MS	F-Value	P-Value	% Cont
Regression	6	14758.3	2459.7	2.94	0.276	—
Temperature	1	3232.7	3232.7	3.86	0.188	31.6
Strain rate	1	1390.2	1390.2	1.66	0.327	13.6
Orientation	1	790.1	790.1	0.94	0.434	7.7
Temperature * Strain rate	1	1510.7	1510.7	1.80	0.311	14.8
Temperature * orientation	1	950.2	950.2	1.13	0.398	9.3
Strain rate * orientation	1	1510.3	1510.3	1.80	0.311	14.8
Error	2	1674.9	837.5			8.2
Total	8	16433.2				100

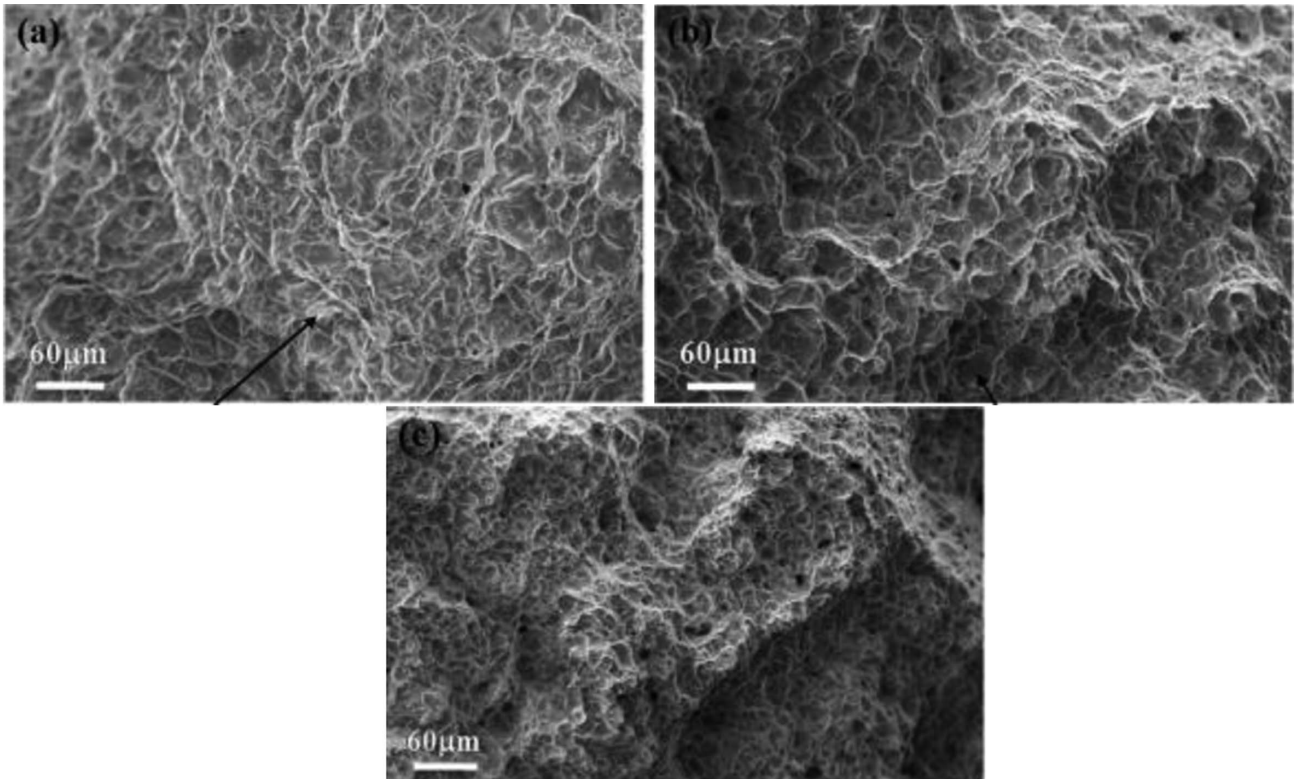

Fig. 4. Zirconium tensile samples fracture surfaces at: (a) 100°C, (b) 150°C and (c) 200°C

TABLE 5

Analysis of Variance of Ultimate Strength

Source	DF	Adj SS	Adj MS	F-Value	P-Value	% Cont
Regression	6	36402.2	6067.0	9.22	0.101	
Temperature	1	4793.0	4793.0	7.29	0.114	48.9
Strain rate	1	991.9	991.9	1.51	0.344	10.1
Orientation	1	548.4	548.4	0.83	0.458	5.6
Temperature * Strain rate	1	1094.7	1094.7	1.66	0.326	11.2
Temperature * orientation	1	670.5	670.5	1.02	0.419	6.8
Strain rate * orientation	1	1045.3	1045.3	1.59	0.335	10.7
Error	2	1315.7	657.9			6.7
Total	8	37717.9				100

TABLE 6

Analysis of Variance for % Elongation

Source	DF	Adj SS	Adj MS	F-Value	P-Value	% Cont
Regression	3	632.852	210.951	45.58	0.000	
Temperature	1	510.235	510.235	110.25	0.000	77.8
Strain rate	1	120.003	120.003	25.93	0.004	18.3
Orientation	1	2.614	2.614	0.56	0.486	0.4
Error	5	23.140	4.628			3.5
Total	8	655.992				100

- Regression Equation for yield strength:

  Yield Strength = 424 – 2.10 Temperature – 8680 Strain rate – 2.01 orientation + 85.9 Temperature * Strain rate + 0.0166 Temperature * orientation – 95.5 Strain rate * orientation

- Regression Equation Ultimate Strength:

  Ultimate strength = 598 – 2.553 Temperature – 7332 Strain rate – 1.68 orientation + 73.2 Temperature * Strain rate + 0.0140 Temperature * orientation – 79.4 Strain rate * orientation

- Regression Equation % Elongation:

  % Elongation = 25.25 + 0.1844 Temperature – 81.7 Strain rate + 0.0147 orientation

4.1. Validation

As shown in Fig. 5, the regression equation was validated at a temperature of 100°C and a strain rate of 0.001s*1. The minimum error in all response parameters was also less than 2%.

5. Conclusion

Zirconium's mechanical properties at various temperatures will be evaluated and characterized using ANOVA. Following are the conclusions drawn from the experimental results.

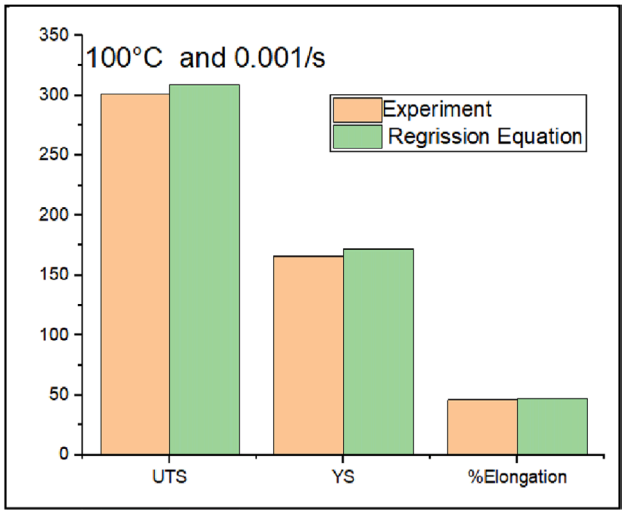

Fig. 5. Regression model validation

- When the temperature rises to 200°C, the flow stress decreases, and the % elongation increases. Higher UTS, YS, and lower % elongation observed at higher deformation rates.
- Scanning electron microscope images showing that the fracture will be ductile for all the temperatures
- The temperature is the most effective parameter with contribution for UTS, YS and % elongation are 41.90,31.60 and 77.80 respectively. The R-squared value for yield strength was found to be 89.91%, for ultimate strength 96.51%, and for elongation 96.47% and less than 2% error was observed during validation.

REFERENCES

[1] N. Ni, D. Hudson, J. Wei, P. Wang, S. Lozano-Perez, G.D. Smith, J.M. Sykes, S.S. Yardley, K.L. Moore, S. Lyon, R. Cottis, Acta Materialia **60** (20), 7132-49 (2012). DOI: https://doi.org/10.1016/j.actamat.2012.09.021

[2] S. Nakamura, H. Harada, S. Raman, P.E. Koehler, Journal of Nuclear Science and Technology **44** (1), 21-8 (2007). DOI: https://doi.org/10.1080/18811248.2007.9711252

[3] H. Stinnertz, Tube Pipe Technol. **1**, 27, 31 (1988).

[4] S. Kosaraju, A. Kalluri, S.K. Singh, A. Haq, ASME 59490 (2019). DOI: https://doi.org/10.1115/IMECE2019-12102

[5] A.U. Haq, A.K. Kavit, T. Rao, T. Buddi, D. Baloji, K. Satyanarayana, S.K. Singh, Materials Today **18**, 4589-97 (2019). DOI: https://doi.org/10.1016/j.matpr.2019.07.433

[6] D. Baloji, K. Anil, K. Satyanarayana, S.K. Singh, M.T. Naik, Materials Today **18**, 4475-81 (2019). DOI: https://doi.org/10.1016/j.matpr.2019.07.417

[7] B. Dharavath, A. ul Haq, M.D. Varma, S.K. Singh, M.T. Naik, Materials Today **26**, 3179-82 (2020). DOI: https://doi.org/10.1016/j.matpr.2020.02.656

[8] S. Miyazaki, H. Kim, Y. Sato, inventors; University of Tsukuba NUC, assignee. patent US 9, 758, 846 (2017).

[9] Y. Zhang, A.A. Volinsky, H.T. Tran, Z. Chai, P. Liu, B. Tian. Journal of Materials Engineering and Performance (10), 3783-8 (2015). DOI: https://doi.org/10.1007/s11665-015-1693-9

[10] F.J. Dunkerley, F. Pledger, V. Damiano, J. Fulton, JOM **3** (11) (1951). DOI: https://doi.org/1003-8.10.1007/BF03397411

[11] A.K. Gupta, H.N. Krishnamurthy, Y. Singh, K.M. Prasad, S.K. Singh, Materials & Design **45**, 616-27 (2013). DOI: https://doi.org/10.1016/j.matdes.2012.09.041

[12] S. Pandre, N. Kotkunde, P. Takalkar, A. Morchhale, R. Sujith, S.K. Singh, Journal of Materials Engineering and Performance **28** (12), 7565-81 (2019). DOI: https://doi.org/10.1016/j.matdes.2012.09.041

[13] N. Kotkunde, A. Badrish, A. Morchhale, P. Takalkar, S.K. Singh, International Journal of Material Forming **13** (3), 355-69 (2020). DOI: https://doi.org/10.1007/s12289-019-01505-3

[14] C.A. Badrish, A. Morchhale, N. Kotkunde, S.K. Singh, Proceedings **1**, 46, 9287-90 (2020). DOI: https://doi.org/10.1016/j.matpr.2020.02.140

[15] B. Dharavath, A. Morchhale, S.K. Singh, N. Kotkunde, M.T. Naik, Journal of Materials Engineering and Performance **29** (7), 4766-78 (2020). DOI: https://doi.org/10.1007/s11665-020-04968-7

[16] L. Jayahari, P.V. Sasidhar, P.P. Reddy, B. BaluNaik, A.K. Gupta, S.K. Singh, Journal of King Saud University-Engineering Sciences **26** (1), 21-31 (2014). DOI: https://doi.org/10.1016/j.jksues.2012.12.006

[17] L Jayahari, B.B. Naik, S.K. Singh, Procedia Materials Science **6**, 115-22 (2014). DOI: https://doi.org/10.1016/j.mspro.2014.07.013

[18] B. Dharavath, A. ul Haq, T. Buddi, S.K. Singh , M.T. Naik, Advances in Materials and Processing Technologies **6** (2), 384-95 (2020). DOI: https://doi.org/10.1080/2374068X.2020.1728648

[19] G. Mahalle, N. Kotkunde, A.K. Gupta, R. Sujith, S.K. Singh, Y.C. Lin, Journal of Materials Engineering and Performance **28** (6), 3320-31 (2019). DOI: https://doi.org/10.1007/s11665-019-04116-w

[20] Y.C. Lin, H. Yang, X.M. Chen, D.D. Chen, Advanced Engineering Materials (8), 1800234 (2008). DOI: https://doi.org/10.1002/adem.201800234